Flow Around Curved Plates at Low Subcritical Reynolds Number: Investigation of Wake Characteristics

Amala Anil, K. ArunKumar, R. Ajith Kumar, C. M. Hariprasad and Thamil Mani

Abstract In this paper, numerical simulation results of flow over flat plate and curved plates at a Reynolds number of 8000 are presented. Drag coefficient and Strouhal number trends are reported at different chord length (CL)-to-diameter (*D*) ratios of 0, 6/13, 3/4, and 1 with varying angle of incidence (ranging from $\alpha = 0°$ to 30° in steps 10°). The curvature of the plate was adjusted by varying the radius of curvature keeping the chord length fixed at 40 mm. The results of this study show that the aerodynamic characteristics, viz., drag force and Strouhal number, are significantly affected by the introduction of curvature and flow angle of incidence (plate orientation). The maximum reduction of drag coefficient obtained is 58% by the introduction of both plate curvature and plate orientation. Further, it is noted that base pressure coefficient complies with the trend of the drag and the maximum flow field vorticity shows an abrupt increase in CL/*D* beyond 6/13.

Keywords Plate curvature · Flow incidence angle · Aerodynamic characteristics · Coefficient of drag · Strouhal number · Base pressure coefficient · Vorticity magnitude

A. Anil (✉) · K. ArunKumar · R. Ajith Kumar · C. M. Hariprasad · T. Mani
Department of Mechanical Engineering, Amrita Vishwa Vidyapeetham, Amritapuri, India
e-mail: amalaanili47@gmail.com

K. ArunKumar
e-mail: akmallasseril@gmail.com

R. Ajith Kumar
e-mail: amritanjali.ajith@gmail.com

C. M. Hariprasad
e-mail: hariology@yahoo.co.in

T. Mani
e-mail: thamilthedal@gmail.com

P. Saha et al. (eds.), *Advances in Fluid and Thermal Engineering*,
Lecture Notes in Mechanical Engineering,
https://doi.org/10.1007/978-981-13-6416-7_76

Nomenclature

CL	Chord length of the plate
U	Uniform flow velocity
C_{pb} (base pressure coefficient)	$\frac{P_b - P_\infty}{\frac{1}{2}\rho U^2}$
C_l (lift coefficient)	$\frac{2F_l}{\rho A U^2}$
P_b	Base pressure
F_l	Lift force
ζ_{max}	Maximum value of vorticity
g	Acceleration due to gravity
f_s	Vortex shedding frequency
D	Diameter of plate
CL/D	Chord length-to-diameter ratio
C_d (drag coefficient)	$\frac{2F_d}{\rho A U^2}$
F_d	Drag force
P_∞	Pressure at uniform flow field
μ	Dynamic viscosity
St (Strouhal number)	$\frac{f_s D}{U}$
A	Cross-sectional area

1 Introduction

Flow characteristics of a bluff body have been extensively investigated in the past few years due to its wide variety of engineering applications. Among the bluff bodies, a flat plate is one with possibly the simplest configuration. Few works were reported on flow over flat plates.

Modi et al. [1] investigated the effect of blockage ratio on the aerodynamic characteristics of a flat plate in a subcritical Reynolds number range. Authors reported that increase in the blockage ratio will result in an enhancement of drag and lift. Lisoski [2] discussed the effect of flat plate thickness by representing a curve of the drag coefficient as a function of plate thickness, wherein an increment of drag coefficient with plate thickness was noted. Xu et al. [3] experimentally investigated the flow over corner modified flat plate and concluded that front-edge modification of flat plate will lead to a reduction of wake width and coefficient of drag. Further, Chen and Fang [4] conducted wind tunnel tests on the flat plate with beveled sharp edges to discuss the relation between Strouhal number and angle of attack. Through flow visualization, Radhakrishnan [5] explained the mechanism behind the origin and size manipulation of twin vortices that shed from a flat plate and the relation of reverse flow location with the Reynolds number.

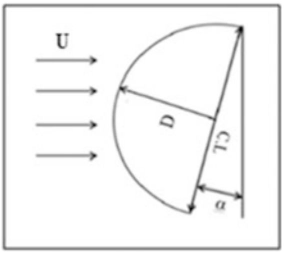

Fig. 1 Model geometry and test configuration

Sharma et al. [6] reported that it is possible to control the size of the vortex shed from flat and also curved plates changing its orientation to the flow. Balu et al. [7] experimentally analyzed vortex length, vortex size, and Strouhal number in flow over curved plates at a subcritical Reynolds number of 5878. They found that by the introduction of curvature and angle of incidence, the wake vortex characteristics can be considerably manipulated. Damu et al. [8] numerically investigated flow over flat plate and curved plates with varying diameter and orientation. They found that an increase in the angle of incidence leads to a reduction of the coefficient of drag. However, their results are expected to be notably influenced by the higher blockage ratio ($\sim$17%) set in their simulations.

The objective of the present study is to numerically investigate the effect of curvature (convex) and orientation in the aerodynamic characteristics of a plate placed in water flow at a Reynolds number of 8000 (based on CL). The chord length-to-diameter ratios (CL/*D*) selected for the study are 0 (flat plate), 6/13, 3/4, and 1. For all the plates, constant chord length (CL) of 40 mm was maintained and angle of incidence (α) was varied from 0° to 30° in steps of 10°. The test configuration for the simulation is shown in Fig. 1. Care is taken to keep the model blockage as low as 3.8% so as to avoid its influence.

2 Computational Model and Validation

ANSYS Fluent 14.0 was used for the computational analysis. Turbulent flow is analyzed by SST k–ω model for better vortex capture. First-order upwind scheme was used for convective and diffusive terms. The fluid medium considered is water, and free stream turbulence intensity was taken as 1%. The blockage ratio had set to be 3.8%. Figure 2 shows the details of the computational domain considered in the present study.

The governing equations for a 2D incompressible flow are as follows

$$\text{Continuity equation } \partial\rho/\partial t + \nabla.(\rho U) = 0 \quad (1)$$

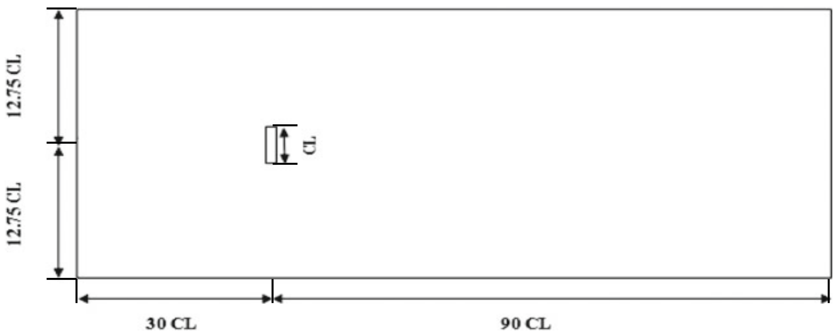

Fig. 2 Computational domain

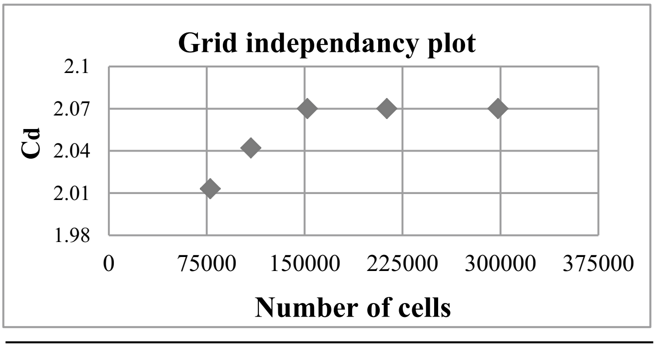

Fig. 3 Grid independency plot

$$\text{Momentum equation } \rho(\partial U/\partial t) + \rho U\nabla.U = -\nabla P + \mu\nabla^2 U + \rho g \tag{2}$$

Grid independency test is carried out for five different sizes of the grid in the same computational domain of flat plate. From Fig. 3, it was seen that the mean drag coefficient becomes a constant value of 2.07 beyond 150,000 cells. Hence, the number of cells is chosen as 150,000 for saving memory and computational time.

The numerical simulation requires validation to be carried out. In this study, flat plate kept normal to the flow, the numerically obtained values of C_d and *St* complies with those reported in the literature at Reynolds number = 8000. Till now, no literature results are available for validating curved plate at this Reynolds number range. So, results for curved plate (CL/*D* = 1) were validated using the experimental results obtained employing a three-component force-balancing mechanism in a subsonic wind tunnel in the Aerodynamics Laboratory of Amrita School of Engineering at Amritapuri Campus. Figure 4 shows the curved plate mounted in the wind tunnel. Validation results are shown in Table 1.

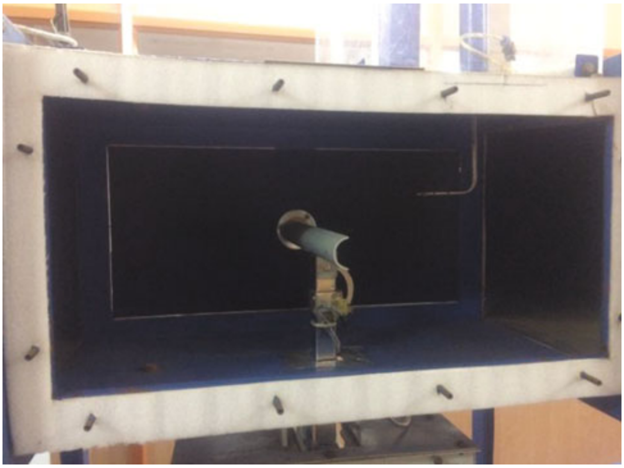

Fig. 4 Curved plate mounted in the test section of wind tunnel

Table 1 Comparison of values obtained in the present study with experimental values for flat plate and curved plate (CL/*D* = 1)

Geometry	Aerodynamic characteristics	Experimental values	Present study
Flat plate (CL/*D* = 0)	C_d	2.07 [1]	2.07
	St	0.149 [1]	0.15
Curved plate (CL/*D* = 1)	C_d	1.13 [Wind tunnel result]	1.07

3 Results and Discussion

The aerodynamic drag coefficient, Strouhal number, base pressure coefficient, and magnitude of maximum flow field vorticity were numerically obtained for all the models having 40-mm chord length kept normal to the flow. The simulations were carried out for all the CL/*D* ratios by varying the angles of incidence in steps of 10° up to 30°.

3.1 Coefficient of Drag (C_d)

Figure 5a shows the typical time series of drag coefficient for CL/*D* = 1.0 at α = 0° from which the mean drag coefficient value is estimated. Similarly, mean C_d values for other models were taken from their respective time series at all flow angles of

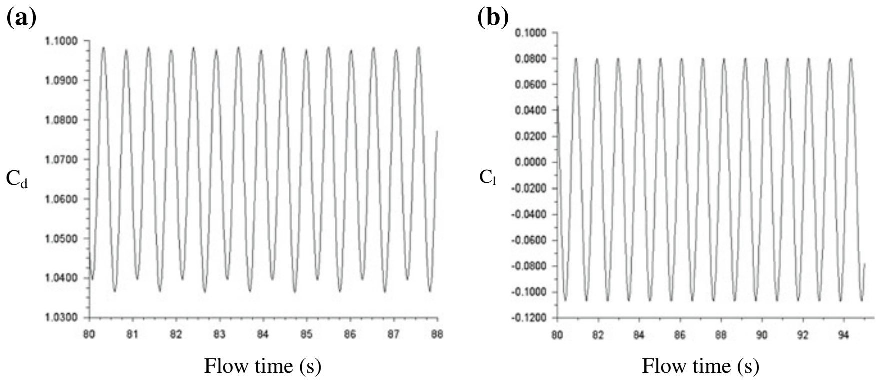

Fig. 5 Time series of $C_{\rm d}$ and $C_{\rm l}$ for the curved plate with CL/*D* = 1 at $\alpha = 0°$

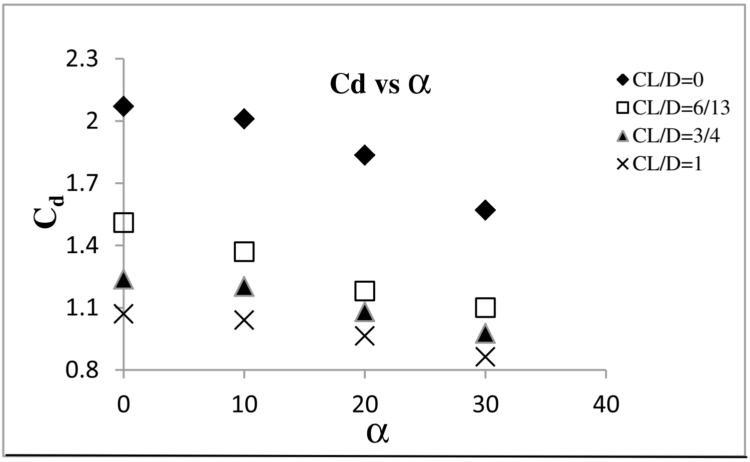

Fig. 6 Variation of drag coefficient versus angle of incidence

incidence. Figure 6 shows the variation of mean drag coefficient of all the CL/*D* models at different angles of attack. For all the models, coefficient of drag shows a decreasing trend when the angle of incidence increases. It could also be seen that, for a given value of α, Cd decreases with increase in CL/*D* ratio. The same declining trend is obtained for lift (rms) coefficient w.r.t. CL/*D* (but not presented here due to space constraints). Compared to all other CL/*D* ratios, the curved plate of CL/*D* = 6/13 shows a maximum reduction of 27% at 30° incident angle. Also from Fig. 6, it is clear that the effect of plate curvature is comparatively less at 30° incident angle. The maximum value of $C_{\rm d}$ was obtained on flat plate at 0° incidence, viz., 2.07 which is close to that of a square cylinder [9]. Considering both the plate curvature and the plate orientation, a total reduction of drag of about 58% is achieved as revealed in Fig. 6.

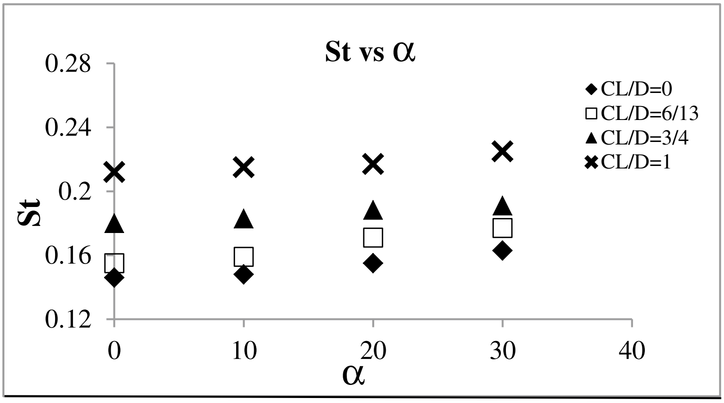

Fig. 7 Strouhal number variation for different models at different incidence angles

*3.2 Strouhal Number (*St*)*

Figure 7 shows the Strouhal number variation for all CL/*D* models at different angles of incidence. The inverse of the time between two adjacent troughs from the lift time series (see Fig. 5b) is used to calculate the vortex shedding frequency which in turn gives the Strouhal number for each case. It can be seen that St registers a very gradual increase with an increase in angle of incidence for all the models. Comparing with Fig. 6, the trends of *St* and C_d show that there exists a near-inverse relationship between them as revealed for bluff bodies in the literature [10]. Strouhal number value is the maximum for the model with CL/*D* = 1 at 30° incidence and is minimum for the flat plate at 0°. This is due to the fact that, when CL/*D* ratio increases, the body will become more streamlined wherein the upper and lower shear layers become close to each other facilitating closer interaction between the shear layers thereby speeding up the shedding process.

3.3 Coefficient of Base Pressure (C_{pb}*)*

In Fig. 8, C_{pb} values for all models are reported at the angle of incidence 0°. From the figure, it can be observed that $-C_{pb}$ is having a decreasing trend with the introduction of curvature. Base pressure coefficient has got the maximum negative value (or minimum positive value) for flat plate at 0°, so the value of drag coefficient is the highest for the same. This could be attributed to the larger wake width for the flat plate (CL/*D* = 0) for which the separation points are fixed. The maximum increase of base pressure coefficient (decrease of negative C_{pb}) w.r.t the CL/D ratio is found to be around 24%.

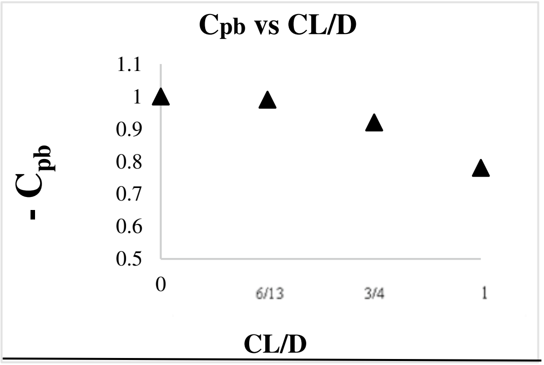

Fig. 8 Variation of C_{pb} with different CL/*D* ratios at $\alpha = 0°$

3.4 Vorticity Magnitude (ζ)

Vorticity is twice the angular velocity vector for the rotating fluid. The maximum value of vorticity magnitude occurs at $x/D = 2.25$ and $y/D = 0.32$ in the flow domain for all models kept normal to the flow ($\alpha = 0°$); '*x*' and '*y*' are measured from the body center along the wake centerline. From Fig. 9, it can be observed that ζ_{max} shows an increasing trend with the introduction of curvature. ζ_{max} abruptly increases for CL/*D* beyond 6/13, and the maximum value was observed for the curved plate with CL/*D* = 1. Maximum vorticity increases by about 6%.

In general, the observed aerodynamic features described in Figs. 3, 5, 6, 7, and 8 could be attributed to the change in the shear layer configuration and corresponding changes in the wake vortex structures around the body when the plate curvature and flow incidence angle are changed.

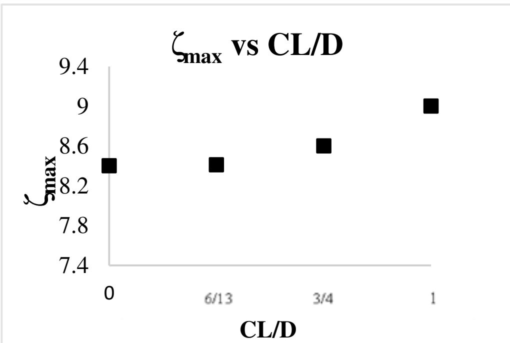

Fig. 9 Variation of C_{pb} with different CL/*D* ratios at $\alpha = 0°$

4 Conclusions

From the numerical simulation and analysis performed in this study, the following conclusions were drawn.

1. It is observed that there is a significant drag variation for a plate by varying its curvature and orientation to the flow. The coefficient of drag decreases with respect to an increase in both flow incidence angle and CL/D ratio. The drag value is found to be minimum for the model with CL/*D* ratio = 1.0 at an angle of 30° with a corresponding drag reduction of about 20%. Considering both plate curvature and its orientation, a total reduction of 58% could be achieved in the drag value which is a notable highlight in the present results.
2. For all the models, Strouhal number is found to exhibit a gradual increase with an increase in the incidence angle and exhibits a near-inverse relationship with the drag coefficient.
3. The maximum flow field vorticity is found to increase w.r.t the CL/*D* ratio beyond CL/*D* = 6/13.

References

1. Modi VJ, EL-Sherbiny SE (1977) A free-streamline model for bluff bodies in confined flow. J Fluids Eng 99(3):585–592
2. Lisoski DLA (1993) Nominally 2-dimensional flow about a normal flat plate. Dissertation (Ph.D.), California Institute of Technology
3. Xu Y-Z, Feng L-H, Wang J-J (2015) Experimental Investigation on the flow over normal flat plates with various corner shapes. J Turbul 16(7):607–616
4. Chen JM, Fang Y-C (1996) Strouhal number of inclined flat plate. J Wind Eng Ind Eng 61 (3):99–112
5. Rathakrishnan E (2012) Visualization of the flow field around a flat plate. IEEE Instrum Measur Magaz 15
6. Sharma H, Vashishtha A, Rathakrishnan E (2008) Twin-vortex flow physics. J Aerosp Eng 222:783–788
7. Balu Haridas, Ajith kumar R, Arunkumar K (2016) Vortex manipulation in flow over curved plates. In: Proceedings of the 43th national conference on fluid mechanics and fluid power
8. Damu Murali, Arunkumar K, Ajith Kumar R, Srikrishnan AR (2017) Flow past a curved plate: analysis of drag coefficient and Strouhal number. In: Proceedings of the 44th national conference on fluid mechanics and fluid power
9. Yen SC, Yang CW (2011) Flow patterns and vortex shedding behavior behind a square cylinder. J Wind Eng Ind Aerodyn 99(8):868–878
10. Ahlborn B, Seto ML, Noack BR (2002) On drag, Strouhal number and vortex-street structure. J Fluid Dyn Res 30(6):379–399